Molecular Crystals and Liquid Crystals
Publication details, including instructions for authors and subscription information:
http://www.tandfonline.com/loi/gmcl20

Reversible Heat-Induced Microwrinkling of PEDOT:PSS Nanofilm Surface Over a Monodomain Liquid Crystal Elastomer

Francesco Greco [a], Valentina Domenici [b], Stefano Romiti [a c], Tareq Assaf [a d], Blaž Zupančič [e f g], Jerneja Milavec [e], Boštjan Zalar [e f g], Barbara Mazzolai [a] & Virgilio Mattoli [a]

[a] Center for Micro-BioRobotics @ SSSA, Istituto Italiano di Tecnologia, Pontedera, Italy

[b] Dipartimento di Chimica e Chimica Industriale, University of Pisa, Pisa, Italy

[c] Biorobotics Institute, Scuola Superiore Sant'Anna, Pontedera, Italy

[d] Bristol Robotics Laboratory, University of the West of England, Frenchay Campus, Bristol, United Kingdom

[e] Jozef Stefan Institute, Ljubljana, Slovenia

[f] Centre of Excellence NAMASTE, Ljubljana, Slovenia

[g] Centre of Excellence EN-FIST, Ljubljana, Slovenia

Published online: 02 Apr 2013.

To cite this article: Francesco Greco, Valentina Domenici, Stefano Romiti, Tareq Assaf, Blaž Zupančič, Jerneja Milavec, Boštjan Zalar, Barbara Mazzolai & Virgilio Mattoli (2013) Reversible Heat-Induced Microwrinkling of PEDOT:PSS Nanofilm Surface Over a Monodomain Liquid Crystal Elastomer, Molecular Crystals and Liquid Crystals, 572:1, 40-49, DOI: 10.1080/15421406.2012.763208

To link to this article: http://dx.doi.org/10.1080/15421406.2012.763208

Mol. Cryst. Liq. Cryst., Vol. 572: pp. 40–49, 2013

ISSN: 1542-1406 print/1563-5287 online
DOI: 10.1080/15421406.2012.763208

Reversible Heat-Induced Microwrinkling of PEDOT:PSS Nanofilm Surface Over a Monodomain Liquid Crystal Elastomer

FRANCESCO GRECO,[1] VALENTINA DOMENICI,[2,*] STEFANO ROMITI,[1,3] TAREQ ASSAF,[1,4] BLAŽ ZUPANČIČ,[5,6,7] JERNEJA MILAVEC,[5] BOŠTJAN ZALAR,[5,6,7] BARBARA MAZZOLAI,[1] AND VIRGILIO MATTOLI[1]

[1]Center for Micro-BioRobotics @ SSSA, Istituto Italiano di Tecnologia, Pontedera, Italy
[2]Dipartimento di Chimica e Chimica Industriale, University of Pisa, Pisa, Italy
[3]Biorobotics Institute, Scuola Superiore Sant'Anna, Pontedera, Italy
[4]Bristol Robotics Laboratory, University of the West of England, Frenchay Campus, Bristol, United Kingdom
[5]Jozef Stefan Institute, Ljubljana, Slovenia
[6]Centre of Excellence NAMASTE, Ljubljana, Slovenia
[7]Centre of Excellence EN-FIST, Ljubljana, Slovenia

New bilayered composite systems with tunable and temperature-dependent formation of periodical wrinkles on the surface are the object of this report. The samples were prepared by spin-coating deposition of a thin film of the conducting polymer poly(ethylenedioxythiophene):poly(styrene sulfonate) (PEDOT:PSS) on the surface of standard monodomain liquid crystal elastomer (LCE) films. Several bilayered materials were prepared by changing the thickness of PEDOT:PSS nanofilms. Basic characterization showed very good stability and adhesion between the two components also after performing multiple heat cycles around nematic-to-isotropic transition temperature of the LCE. Interestingly, formation of uniaxially aligned microwrinkles was observed, with most of the wrinkles aligned along perpendicular direction with respect to the nematic director, due to reversible elongation/compression of the LCE during thermal cycles.

Keywords Actuation; bending; composite; conductive polymer; Joule heating; liquid crystal elastomer; PEDOT:PSS; soft actuation; surface; wrinkling

Introduction

Liquid crystal elastomers (LCEs) [1] belong to the class of "shape memory" polymer materials and are object of increasing interest for their potentialities [2] in the field of biomedicine, microrobotics, and optics. The typical actuation mechanism of nematic

*Address correspondence to Valentina Domenici, Dipartimento di Chimica e Chimica Industriale, University of Pisa, via Risorgimento 35, 56126 Pisa, Italy. Tel.: +0039 0502219215; Fax: +0039 0502219260. E-mail: valentin@dcci.unipi.it

LCE films is a thermomechanic one and it is related to the macroscopic elongation observed by decreasing the temperature, so causing a transition from the isotropic to the nematic phase. This shape variation is associated with the alignment of the mesogenic units along a preferred direction, which is defined by the nematic director, n, when entering into the liquid crystalline (nematic) phase. In the recent years, LCE shape variation has been triggered by different external stimuli, such UV-Vis light [3] and electromagnetic fields [4].

Several attempts have been also made to obtain electroactive LCEs, as, for instance, by incorporating inorganic conductive nanomaterials into the LCE matrix. For instance, indirect thermal actuation by Joule heating could be achieved by doping nematic LCE films with carbon nanoparticles [4]. Recently, new composite LCE-based materials [5] have been prepared by embedding in the LCE matrix ferroelectric nanoparticles [6], conductive nanowires [7], and carbon nanotubes [8], resulting in interesting new physical properties and effects, such as the response to infrared laser radiation or the alignment of the nanomaterials at the isotropic-to-nematic phase transition.

Another approach to develop electroactive actuators based on LCEs is the addition to a conductive layer on the top surface of LCE films in order to form bilayered composite materials [9–12]. Despite the main objective of fabricating bilayered LCE-based systems being performance of direct or indirect electroactuation, interesting phenomena occurring at the top surface, such as the formation of tunable microwrinkling and other anisotropic instabilities, have been observed [9,10,12]. Similar periodic surface microstructures have been recently reported for bilayered systems formed by liquid crystalline polymers [13].

The formation of surface wrinkles via thermal stress, pressure, and mechanical stress is a well-known effect occurring on bilayered films formed by two materials having different stiffness and elastic properties [14], and there are also examples in nature, such as the human skin [15]. Recently, there has been an increasing interest in materials science and engineering related to these phenomena of self-organizing surface micro- and nanowrinkling driven by mechanical instabilities, because of the many potential applications of such structured surfaces in the fields of optics, catalysis, biomedicine, metrology, etc. Indeed, the possibility to create surface wrinkles with predesigned patterns and to fine tune, control, and/or measure their wavelengths and amplitudes is of great interest for technological applications, i.e., for the characterization of mechanical properties of nanoscale thin films [16,17] or for the fabrication of artificial biomimetic surfaces, bioinspired photonic and optical grating surfaces [18,19].

In this paper, we report the surface microwrinkling formation on the top surface of a bilayered composite material [9–11] consisting of a first layer made of a monodomain side-chain LCE film and a second layer made of a nanofilm of the conductive polymer poly(ethylenedioxythiophene):poly(styrene sulfonate) (PEDOT:PSS) with a thickness $t \sim 50$ nm. This conductive polymer has been chosen for its excellent stability and mechanical properties [20,21] and for the possibility to fabricate PEDOT:PSS nanofilms of different thicknesses with high level of precision and control [22], starting from its dispersion in water, which allows for using several fabrication/deposition techniques. By testing several different samples at increasing thickness of the PEDOT:PSS layer from 50 nm to several micrometers, we also observed that when the thickness of the PEDOT:PSS layer is large enough (typically $t > 200$ nm), bending actuation instead of wrinkle formation is observed. Thermal actuation via direct Joule heating of the composite materials having a thick PEDOT:PSS layer is also presented together with preliminary testing of prototypes of LCE/PEDOT:PSS bending actuators.

Experimental

Materials

The monodomain nematic LCE films used to make the bilayered systems are polysiloxane side-chain LCEs (see Fig. 1). The preparation of the LCE stripes, following the Finkelmann two-step crosslinking procedure [23], is reported in Refs. [9–11,24]. In particular, data reported in this work refer to the sample EV1–0.20 containing 10% of crosslinking units and remaining percentage of standard mesogenic units (see Fig. 1). This LCE sample was fully characterized in a previous work [24], with a transition temperature between the nematic and the isotropic phase of $T = 73.7^{\circ}$C (determined by differential scanning calorimetry) and the maximum elongation at room temperature about 68% [24,25].

The monodomain LCE samples were cut in small stripes of $\sim$ 2 mm $\times$ 4 mm and exposed to air plasma (80 seconds, power $P = 7$ W; PDC-32G Plasma Cleaner, Harrick Plasma, Ithaca, NY) in order to improve the wettability of their surface by aqueous solutions. A commercially available dispersion of PEDOT:PSS in water (Clevios^{TM} PH1000, 1:2.5 PEDOT:PSS ratio; Heraeus, Hanau, Germany) was employed after filtration and deposited with a micropipette dispenser over the LCE substrate (0.4 μL mm^{-2}). Homogeneous films of PEDOT:PSS were prepared by spin-coating deposition for 60 seonds at 3000 rpm and then drying at room temperature.

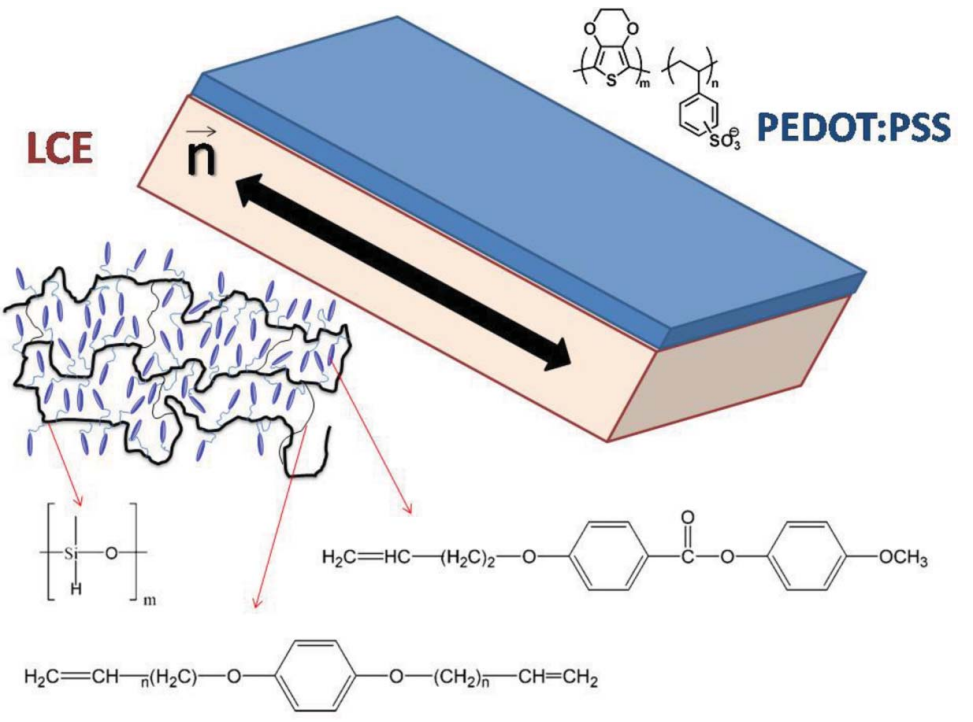

Figure 1. Scheme of the bilayered composite formed by the monodomain LCE film and the nanofilm of PEDOT:PSS. Chemical structure of main components of side-chain LCE and PEDOT:PSS are shown.

In the case of composite samples used for direct Joule heating actuation, PEDOT:PSS conductivity was improved by the introduction of dimethylsulfoxide (DMSO) in the material formulation, since DMSO is known to act as a secondary dopant, improving the conductivity of PEDOT:PSS up to 800–1000 S cm^{-1} [20,21]. A similar recipe as described above was followed: a 5 wt.% content of DMSO was added to Clevios PH1000 and the solution was stirred for 2 hours before filtration. The LCE stripe ($4 \times 1.5 \times 0.3$ mm^3) was exposed to plasma as described above and thin copper wires (diameter 50–170 pm) were placed on it in order to provide wiring for applying voltage to the actuator. Deposition of the conductive layer was then done by drop casting of the solution (0.4 μL mm^{-2}) onto the LCE stripe and the wire, providing a good adhesion and electrical contact between the wire and the conductive layer. The solution was left to dry at room temperature overnight. For bending actuation, the thickness of the PEDOT:PSS layer was about 5 μm. In all cases discussed in the present work, the PEDOT:PSS layer was deposited on the LCE film at room temperature, i.e., in the nematic phase.

Methods

The prepared PEDOT:PSS/LCE composite samples were first characterized in terms of their surface topography, thickness, and electrical properties [11]. Topography of the PEDOT:PSS/LCE composite bilayered system was investigated by scanning electron microscopy (SEM) with a EVO MA 10 ZEISS microscope operating with an accelerating voltage of 10 kV. Thickness of the PEDOT:PSS layer was measured with the aid of a stylus profilometer (P-6 Profilometer; KLA Tencor, Milpitas, CA); as regards nanofilms deposited by spin-coating, thickness measurement was performed on dedicated samples prepared with identical procedures on Si wafer, in order to provide a stable, flat baseline for measurement; as regards thicker films prepared by drop-casting, thickness of the layer was assessed on films prepared as described above on poly(dimethylsiloxane) (PDMS) substrate, detached from its surface after 5–6 hours (films could be easily peeled off due to due to surface hydrophobic recovery of PDMS) and transferred on a clean Si wafer. Electrical resistance of the samples was measured with an LCR meter (LCR E4980A; Agilent, Santa Clara, CA) on sample stripes with 5×6 mm^2 dimension. In order to visualize the thermal actuation of the composite materials, samples were placed on the surface of a Peltier cell, controlled in current by means of a DC power supply, and images of actuation were captured with a digital microscope setup (KH-7700; Hirox, Tokyo, Japan). A thermocouple placed next to the sample was employed to continuously monitor the temperature of the sample. The same experimental setup completed by a dedicated power supply for applying the necessary voltage/current to the sample was used to test actuation of the composite materials via direct Joule heating. Actuation has been tested both in horizontal and in vertical position. Image analysis on pictures taken with the Hirox digital microscope was performed with an image-processing and analysis software (ImageJ).

Results and Discussion

Several PEDOT:PSS/LCE composite samples have been prepared with conductive polymer thickness around 50 nm, as described in the previous section. For convenience, LCE stripes of $4 \times 1.5 \times 0.3$ mm^3 dimension were used. However, we noted that the size and the dimensions of the LCE stripes were not affecting the formation of surface microwrinkling and their periodicity. In Fig. 2, a schematic representation of the mechanism of microwrinkling formation is presented. Since the PEDOT:PSS layer was deposited on the LCE surface at

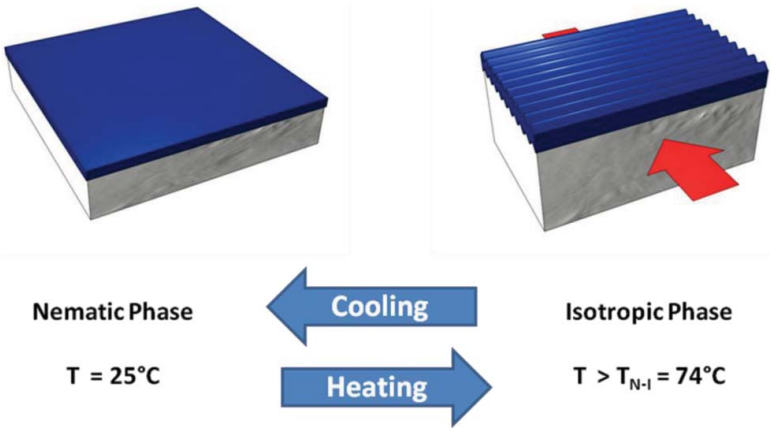

Figure 2. Scheme of the actuation mechanism and wrinkles formation of the bilayered composite by changing the temperature. This mechanism is observed when the PEDOT:PSS conductive polymer is deposited on the LCE surface in the nematic phase (i.e., at room temperature).

room temperature, the formation of microwrinkles is observed when heating up the sample. This was due to the shrinking of the LCE layer when reaching the nematic-to-isotropic transition, $T_{\text{N-I}}$, causing a compression of the top, layer of PEDOT:PSS.

Uniaxially aligned microwrinkles appeared by heating the samples during a first thermal cycle over $T_{\text{N-I}}$. Further cooling and subsequent repeated thermal cycles imposed to the composite sample showed variations in wrinkles periodicity, and the phenomenon was highly reproducible. SEM images (see Fig. 3) were acquired before and after heating the sample in the isotropic phase, and the formation of parallel microwrinkles with temperature-dependent periodicity (wavelength) was observed. In particular, Fig. 3(b) shows that uniaxial microwrinkles were formed and organized in a domain-like arrangement; they were almost all perpendicular to the nematic director, n, i.e., the direction of compression/elongation around $T_{\text{N-I}}$. Optical microscopy images were also collected and analyzed (see, for instance, Fig. 4). As shown both in Fig. 3(b) and Fig. 4, vertical breaks appeared when heating the sample. However, they did not alter the wrinkling wavelength and they remained unaltered after several thermal cycles. As observed by SEM, the PEDOT:PSS nanofilm was submerging at "domain" boundaries, buried deep inside the LCE surface. In fact, some of the ruptures and vertical breaks occurred at "domain" boundaries.

The microwrinkle wavelengths were measured directly by analysis of several images of the PEDOT:PSS/LCE composite by a digital optical microscope (see Fig. 5). The formation of microwrinkles started around $T = 50^{\circ}\text{C}$, and the wavelength rapidly decreased when approaching the $T_{\text{N-I}}$ transition. Above this temperature, the microwrinkle wavelength reached a plateau. The wrinkle wavelength trend reported in Fig. 5 was reproducible after several cycles, and it overlaps with the thermomechanical elongation/contraction of the LCE itself, as previously determined [24]. This reproducible behavior is particularly promising for optical applications, such as formation of tunable optical grating.

Several PEDOT:PSS/LCE composite samples were also prepared with conductive polymer thickness around 5 μm, as described in the previous section. Very good adhesion of the upper PEDOT:PSS layer to the LCE substrate was verified for the composites presented in this work. In fact, no sign of surface delamination or cracking was observed in

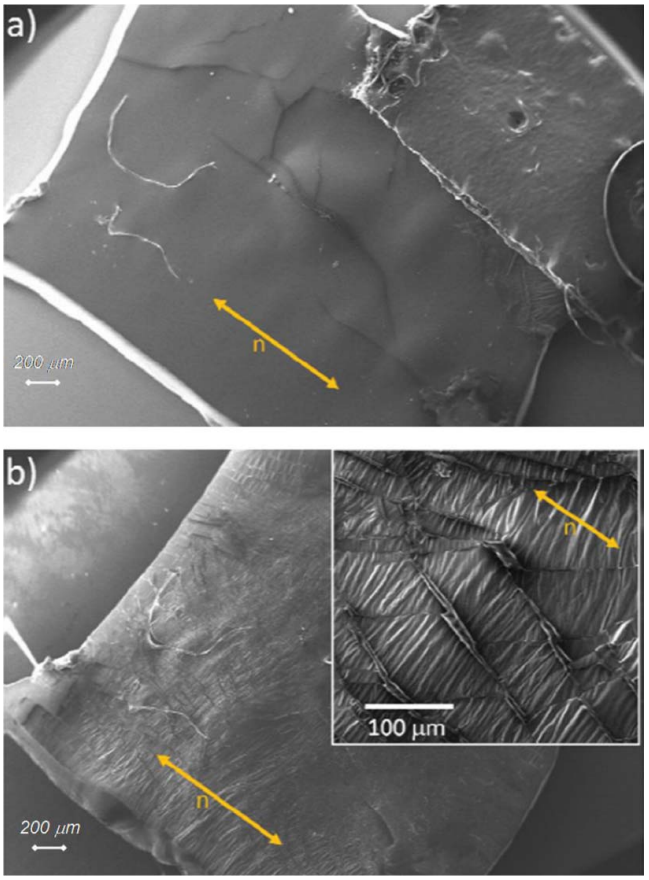

Figure 3. SEM images showing the surface of LCE/PEDOT:PSS composite (a) before and (b) after heating at $T \approx 73^{\circ}$C. Direction defining n director alignment is shown as an orange arrow. Inset at left of image (b) shows a closer view of the surface in which uniaxial microwrinkles are formed and organized in a domain-like arrangement.

any of the prepared samples, due to the good matching of mechanical properties between PEDOT:PSS and the LCE. This behavior is very different from that observed in other polysiloxane materials, such as in the case of PDMS onto which PEDOT: PSS is poorly adhered (see "Methods" section). Different surface chemistry between PDMS and LCE could also play a role in this behavior. The good adhesion between the PEDOT:PSS and the LCE substrates is particularly important for bending actuation and for Joule heating actuation.

An example of bending actuation in horizontal geometry is shown in Fig. 6. Here, the composite sample was laid on a Peltier cell on the LCE side and the temperature was varied in a continuous way from room temperature up to 80°C and reverse. The basic mechanism of bending actuation in this composite structure is related to the combination between the compressive forces due to the contraction of the soft active substrate (LCE), related to the transition of the material from the nematic to the isotropic phase, and the relatively stiffer and incompressible PEDOT:PSS layer.

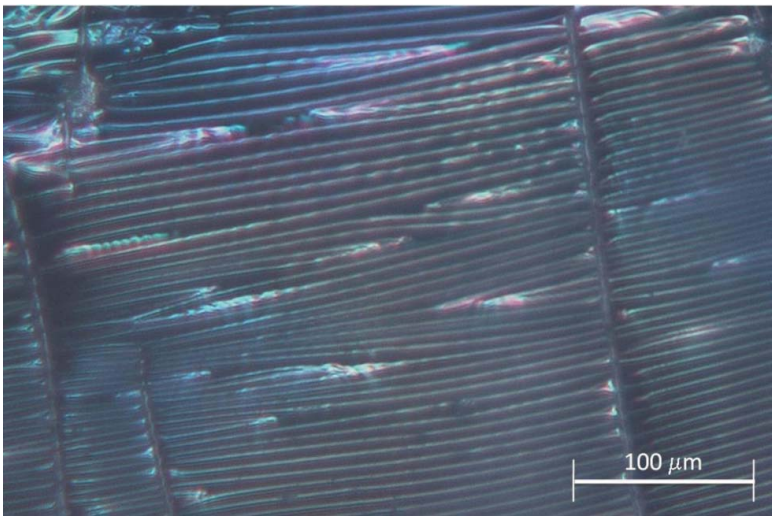

Figure 4. Image of the surface of LCE/PEDOT:PSS composite, observed by an optical microscope. Temperature of the sample is about 75°C, i.e., in the isotropic phase. Horizontal and parallel wrinkles as well as vertical breaks are clearly visible.

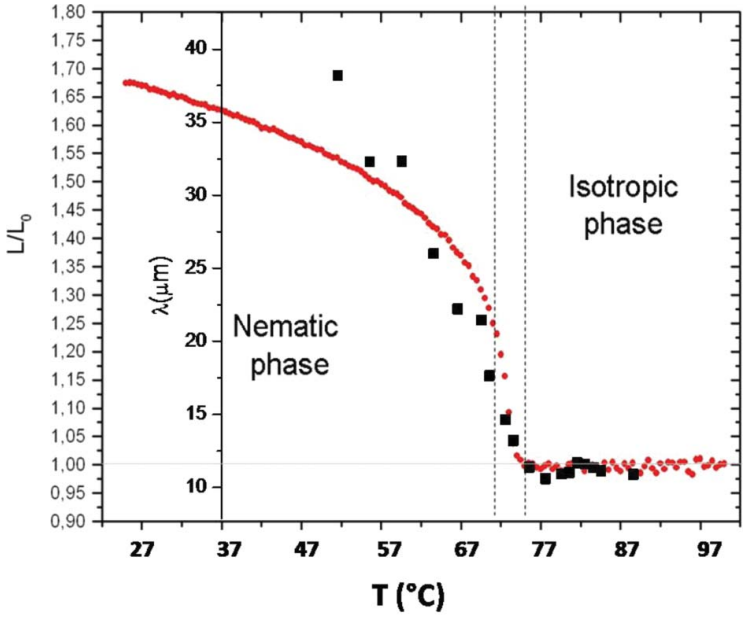

Figure 5. Wrinkles wavelength (λ) as measured by observing several images of PEDOT:PSS/LCE composites by an optical microscope (black squares), during the second cooling process, in the temperature range 90°C–52°C. Thermomechanic elongation (L/L_0) of the pristine LCE film (red circles) at the second cooling run. Vertical dot lines are added in order to put in evidence the isotropic–nematic phase transition.

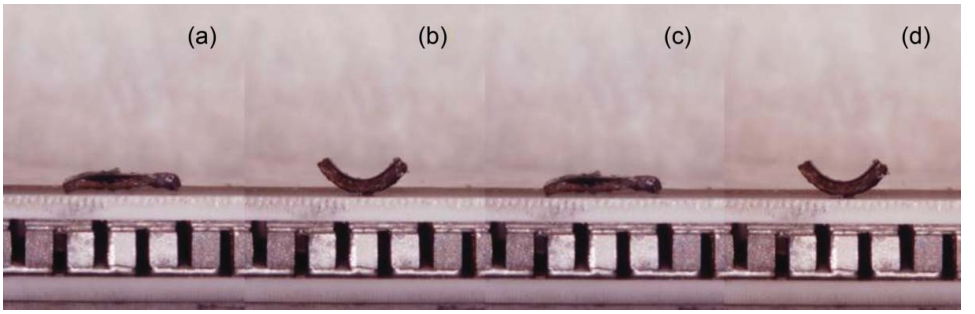

Figure 6. Bending actuation of a PEDOT:PSS/LCE composite prepared at room temperature. Heating of the sample was provided by a Peltier cell controlled under current: (a) and (c) nematic phase; (b) and (d) isotropic phase. Sample size was 4.0 × 2.0 × 0.3 mm^3 and the top PEDOT:PSS layer was 5-μm thick.

As reported in Ref. [11], the thickness of the conductive polymer layer plays a fundamental role in determining the bending of the bilayered system. In particular, if the PEDOT:PSS thickness is below 200 nm, the microwrinkling formation is observed, as reported above. On the contrary, PEDOT:PSS layers thicker than 20–50 μm completely inhibited the LCE actuation, giving rise to irreversible (plastic) deformations or to almost complete blocking of the softer active LCE layer.

A thickness of about 5 μm (as determined by stylus profilometry) was found to be a good compromise in terms of thickness of the PEDOT:PSS layer, both to observe horizontal (Fig. 6) and vertical bending actuation as well as to avoid irreversible deformations. Moreover, given the good electrical properties of the PEDOT:PSS layer, it has been employed for providing localized Joule heating for thermal actuation of the composite (Fig. 7). The resistance of the 5-μm-thick PEDOT:PSS layer was indeed about 30 Ω, as measured by applying a typical voltage of 1.5–3 V [11]. The stability of the PEDOT:PSS/LCE composite

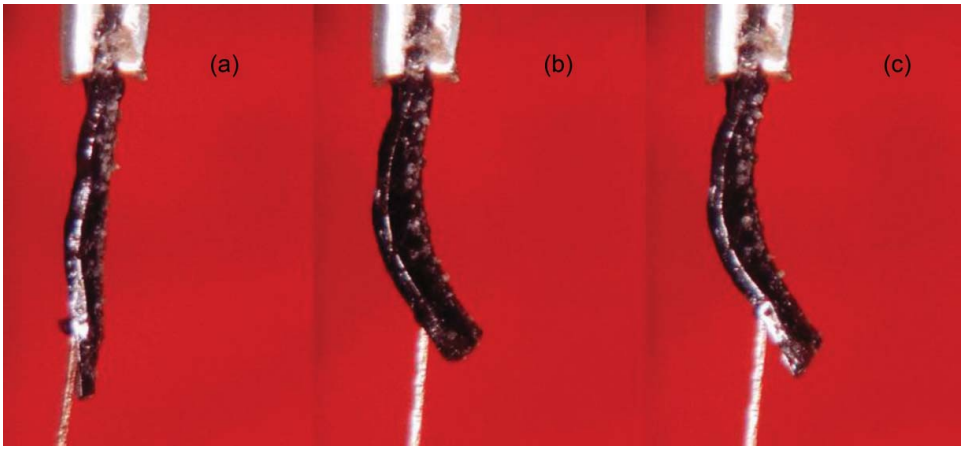

Figure 7. Actuation for the Joule heating effect of a PEDOT:PSS/LCE composite prepared at room temperature: (a) in the nematic phase – first cycle; (b) in the isotropic phase – first cycle; (c) in the isotropic phase – 13th cycle. Sample size was 4.0 × 2.0 × 0.3 mm^3 and the top PEDOT:PSS layer was 5-μm thick.

actuation was tested by measuring the change in resistance as a function of temperature after several cycles of actuation and the reproducibility of data is very high (see, for instance, the actuation for the Joule heating effect at the 1st and 13th cycle in Fig. 7). These preliminary results are very promising and several activities are in progress regarding the optimization of fabrication procedure and design of first prototypes for Joule heating actuation.

Conclusions

In this work, the preparation of new PEDOT:PSS/LCE bilayered composites is reported. Monodomain nematic LCEs were coated with a conductive polymer layer of variable thickness. If the conductive layer was thinner than 200 nm, reversible microwrinkling formation was observed by heating the sample above its nematic-to-isotropic transition temperature, $T_{N\text{-}I}$. Interestingly, reproducible parallel and regularly spaced microwrinkles were formed aligned in perpendicular direction to the nematic director, n, i.e., to the direction of compression/elongation of the LCE sample. Wrinkles were retained upon cooling and for subsequent thermal cycles, with wrinkles periodicity varying with temperature in a reproducible way. By increasing the thickness of the PEDOT:PSS layer, bending of the bilayer was produced instead of microwrinkling. A prototype of Joule heating actuator is also reported. The bilayered composites here described showed high potentialities as optical tunable grating surfaces and for the measurement of mechanical properties, such as elastic moduli in thin films and nanomaterials.

Acknowledgments

The authors are grateful to COST (European Cooperation in Science and Technology) in the framework of ESNAM (European Scientific Network for Artificial Muscles) – COST Action MP1003. JM thanks the COST ACTION MP1003 for the short-term scientific mission STSM-MP1003–9391. VD thanks the Centre of Excellence NAMASTE (Ljubljana, Slovenia) for the financial support as visiting professor in 2011.

References

[1] Warner, M., & Terentjev, E. M. (2003). *Liquid Crystal Elastomers*, Oxford University Press: Oxford.
[2] Ohm, C., Brehmer, M., & Zentel, R. (2010). *Adv. Mater.*, *22*, 3366.
[3] Yu, Y., Nakano, M., & Ikeda, T. (2003). *Nature London*, *425*, 145.
[4] Chambers, M., Finkelmann, H., Remskar, M., Sanchez-Ferrer, A., Zalar, B., & Zumer, S. (2009). *J. Mater. Chem.*, *19*, 1524–1531.
[5] Ge, Q., Luo, X. F., Rodriguez, E. D., Zhang, X., Mather, P. T., Dunn, M. L., & Qi, H. J. (2012). *J. Mech. Phys. Solid*, *60*, 67–83.
[6] Domenici, V., Zupancic, B., Laguta, V. V., Belous, A. G., V'yunov, O. I., Remskar, M., & Zalar, B. (2010). *J. Phys. Chem. C*, *114*, 10782–10789.
[7] Domenici, V., Conradi, M., Remskar, M., Virsek, M., Zupancic, B., Mrzel, A., Chambers, M., & Zalar, B. (2011). *J. Mater. Sci.*, *46*, 3639–3645.
[8] Ji, Y., Marshall, J. E., & Terentjev, E. M. (2012). *Polymers*, *4*, 316–340.
[9] Domenici, V., Greco, F., Mattoli, V., Zalar, B., Zupancic, B., Assaf, T., & Romiti, S. (2011). Reversible heat-induced microwrinking of PEDOT:PSS nanofilm surface over a monodomain Liquid Crystal Elastomer. Oral contribution presented at 6th International Liquid Crystal Elastomer Conference, ILCEC2011, September 6, Lisbon, Portugal.

[10] Romiti, S. (2012). *New actuators based on liquid crystal elastomers and conductive polymers*. Master's thesis, University of Pisa, Italy.
[11] Greco, F., Domenici, V., Assaf, T., Romiti, S., & Mattoli, V. (2012). *Proceedings of the Fourth IEEE RAS/EMBS International Conference on Biomedical Robotics and Biomechatronics*. Article number 6290942, Pages 646–651. New York: IEEE.
[12] Agrawal, A., Luchette, P., Palffy-Muhoray, P., Biswal, S. L., Chapman, W. G., & Verduzco, R. (2012). *Soft Matter*, *8*, 3138.
[13] Kang, S. H., Na, J. H., Moon, S. N., Lee, W. I., Yoo, P. J., & Lee, S. D. (2012). *Langmuir*, *28*, 3576–3582.
[14] Chen, C. M., & Yang, S. (2012). *Polymer Inter.*, *61*, 1041–1047.
[15] Cerda, E., & Mahadevan, L. (2003). *Phys. Rev. Lett.*, *90*, 074302.
[16] Harris, A., Wild, P., & Stopak, D. (1980). *Science*, *208*, 177–179.
[17] Chung, J. Y., Nolte, A. J., & Stafford, C. M. (2011). *Adv. Mater.*, *23*, 349–368.
[18] Wu, D., Chen, Q.-D., Xia, H., Jiao, J., Xu, B.-B., Lin, X.-F., Xu, Y., & Sun, H.-B. (2010). *Soft Matter*, *6*, 263–267.
[19] Stafford, C. M., Harrison, C., Beers, K. L., Karim, A., Amis, E. J., Vanlandingham, M. R., Kim, H. C., Volksen, W., Miller, R. D., & Simonyi, E. E. (2004). *Nature Mater.*, *3*, 545–550.
[20] Na, S.-I., Wang, G., Kim, S.-S., Kim, T.-V., Oh, S.-H., Yu, B.-K., Lee, T., & Kim, D. W. (2009). *J. Mater. Chem.*, *19*, 9045–9053.
[21] Dimitriev, O. P., Grinko, D. A., Noskov, Yu. V., Ogurtsov, N. A., & Pud, A. A. (2009). *Synthetic Metals*, *159*, 2237–2239.
[22] Greco, F., Zucca, A., Taccola, S., Menciassi, A., Fujie, T., Haniuda, H., Takeoka, S., Dario, P., & Mattoli, V. (2011). *Soft Matter*, *7*, 10642–10650.
[23] Kupfer, J., & Finkelmann, H. (1991). *Macromol. Rapid Commun.*, *12*, 717–726.
[24] Domenici, V., & Zalar, B. (2010). *Phase Trans.*, *83*, 1014–1025.
[25] Domenici, V. (2012). *Prog. Nucl. Mag. Res. Sp.*, *63*, 1–32.